

O *K*-edge and Cu *L*₂₃-edge XANES study on the concentration and distribution of holes in the (Pb_{2/3}Cu_{1/3})₃Sr₂(Y, Ca)Cu₂O_{8+z} superconductive phase

M. Karppinen* and M. Kotiranta

Laboratory of Inorganic and Analytical Chemistry, Helsinki University of Technology, FIN-02015 Espoo, Finland

H. Yamauchi

Materials and Structures Laboratory, Tokyo Institute of Technology, Yokohama 226-8503, Japan

P. Nachimuthu and R. S. Liu

Department of Chemistry, National Taiwan University, Taipei, Taiwan, Republic of China

J. M. Chen

Synchrotron Radiation Research Center (SRRC), Hsinchu, Taiwan, Republic of China

(Received 28 August 2000; published 17 April 2001)

By means of high-resolution O *K*-edge and Cu *L*₂₃-edge x-ray absorption near-edge-structure spectroscopy continuous increase of the CuO₂-plane hole concentration with increasing Ca-substitution level has been established for the superconductive, oxygen-depleted ($z \approx 0$) (Pb_{2/3}Cu_{1/3})₃Sr₂(Y_{1-x}Ca_x)Cu₂O_{8+z} [(Pb_{2/3}Cu_{1/3})-3212] phase with a three-layer PbO-Cu-PbO charge-reservoir block. For the O *K*-edge absorption, a pre-edge peak at ~ 528.3 eV is seen, originating from the excitation of the O *1s* electron to the O *2p* hole state located in the CuO₂ plane. With increasing Ca-substitution level, the intensity of this peak continuously increases within the substitution range studied, i.e., $0 \leq x \leq 0.5$. Consistently, with increasing x , the shoulder on the high-energy side of the main absorption peak at ~ 932.0 eV in the Cu *L*₂₃-edge spectra, i.e., a feature typically assigned to formally trivalent copper, enhances. From the Cu *L*₂₃-edge spectra it was furthermore confirmed that the charge-reservoir copper remains in the monovalent state, indicating that the holes created through Ca substitution are directed solely into the superconductive CuO₂ plane. In terms of increasing the CuO₂-plane hole concentration, Ca substitution was found to work more efficiently in (Pb_{2/3}Cu_{1/3})-3212 as compared to, e.g., the related Bi-2212 phase.

DOI: 10.1103/PhysRevB.63.184507

PACS number(s): 74.62.Dh, 61.10.Ht, 74.72.Jt

I. INTRODUCTION

In the layered structures of superconductive copper oxides, $M_m A_2 Q_{n-1} Cu_n O_{m+2+2n\pm\delta} [M-m2(n-1)n]$, the superconductive block, CuO₂-(Q-CuO₂)_{n-1} is sandwiched by AO layers and $M_m O_{m\pm\delta}$ “charge-reservoir” blocks forming a layer sequence, AO-CuO₂-(Q-CuO₂)_{n-1}-AO-(MO_{1±δ'})_m.¹ Even though the CuO₂-plane hole concentration is known to crucially control the superconductivity characteristics, determination of the local hole concentration of individual CuO₂ planes and MO_{1±δ'} layers, i.e., the distribution of holes among the different layers over the unit cell, has remained an unsolved problem for most of the known $M-m2(n-1)n$ phases. In the case of, e.g., Bi-, Pb-, Tl-, Hg- and Cu- $m2(n-1)n$ superconductors, one of the uncertainties arises from the fact that, besides the CuO₂-plane Cu, also the charge-reservoir constituent M is likely to possess a mixed-valence value. The x-ray absorption near-edge structure (XANES) technique provides us with a direct probe for investigating the local concentration of holes at the distinct copper and oxygen sites in superconductive copper-oxide phases. So far, XANES measurements—both O *K*-edge and Cu *K*- and *L*₂₃-edge studies—have been most intensively applied for establishing changes in site-specific hole concentrations of the CuA₂QCu₂O_{6+z} or Cu-1212 phase, i.e., the distribution of

holes among the superconductive CuO₂ plane and the charge-reservoir CuO_z chain, with varying cation-substitution level and/or oxygen content.^{2–10} Note that, Cu-1212 is nothing but the so-called “123” phase. Also note that in the present contribution “ z ” is used instead of “ $1 - \delta$ ” for the amount of excess oxygen. The original assignment of the multiple pre-edge peaks in the O *K*-edge spectra originating from the different binding energies of O *1s* levels of unequivalent oxygen sites is based on the single-crystal study of Nücker *et al.*,² but powder samples have since then been successfully characterized as well. Also for the Bi₂Sr₂(Y_{1-x}Ca_x)Cu₂O_{8+δ} or Bi-2212 phase, it was recently demonstrated that the intensity of the pre-edge peak around 528 eV in the O *K*-edge XANES spectrum corresponds to the concentration of holes created in the CuO₂ plane with increasing Ca-substitution level.¹¹

From the crystal- and redox-chemical points of view, (Pb_{2/3}Cu_{1/3})₃A₂(R,Ca)Cu₂O_{8+z} [(Pb_{2/3}Cu_{1/3})-3212] (Refs. 12, 13) is one of the most interesting superconductive copper-oxide phases. The structure of the (Pb_{2/3}Cu_{1/3})-3212 phase with a layer sequence, AO-CuO₂-(R,Ca)-CuO₂-AO-PbO-CuO_z-PbO, differs from that of Cu-1212 with respect to the number of charge-reservoir layers m .^{14–17} That is, in (Pb_{2/3}Cu_{1/3})-3212 the single nonstoichiometric CuO_z layer, which is the only charge-reservoir constituent in Cu-1212, is sandwiched by

two oxygen-stoichiometric PbO planes. Synthesis in an atmosphere of a low-oxygen partial pressure results in an oxygen-deficient phase with $z < 0.1$, but like Cu-1212, the $(\text{Pb}_{2/3}\text{Cu}_{1/3})$ -3212 lattice easily accommodates oxygen atoms around the charge-reservoir Cu atom when annealed in an O_2 -rich atmosphere. Oxygen loading up to $z \approx 1.8$ is possible without destroying the structure, though no intermediate oxygen configurations between the lowest and the highest values exist.^{16–18} In $(\text{Pb}_{2/3}\text{Cu}_{1/3})$ -3212, the holes that are created in the charge-reservoir block upon the entering of excess oxygen atoms in the structure, are not transferred into the CuO_2 -(R ,Ca)- CuO_2 block but are believed to be trapped on Pb and Cu in the $\text{PbO-CuO}_2\text{-PbO}$ charge reservoir. In other words, oxygen loading seems to increase the oxidation states of the charge-reservoir cations only, from +I to +II for Cu and from +II to +IV for Pb, as suggested by the results of both BVS calculations^{15,17,19} and wet-chemical analyses.^{20,21} This conclusion manifests itself by the fact that the oxygenated $(\text{Pb}_{2/3}\text{Cu}_{1/3})$ -3212 phase does not superconduct. Also with the oxygen-deficient configuration at $z \approx 0$, $(\text{Pb}_{2/3}\text{Cu}_{1/3})$ -3212 is an antiferromagnetic semiconductor if the Q -metal layer between the two CuO_2 planes in the CuO_2 - Q - CuO_2 block is composed of rare-earth element(s) only.²² Only when substituting part of the trivalent R ions by divalent Ca, superconductivity arises.

In the present paper, the continuous generation of holes into the CuO_2 plane with an increasing Ca-substitution level in the oxygen-deficient $(\text{Pb}_{2/3}\text{Cu}_{1/3})_3\text{Sr}_2(\text{Y}_{1-x}\text{Ca}_x)\text{Cu}_2\text{O}_{8+z}$ phase has been followed for the first time directly by means of O K -edge and Cu L_{23} -edge XANES measurements. From the Cu L_{23} -edge spectra, it could furthermore be confirmed that the charge-reservoir Cu atom remains at the monovalent state throughout the Ca-substitution range studied ($0 \leq x \leq 0.5$).

II. EXPERIMENT

Six powder samples of the $(\text{Pb}_{2/3}\text{Cu}_{1/3})_3\text{Sr}_2(\text{Y}_{1-x}\text{Ca}_x)\text{Cu}_2\text{O}_{8+z}$ phase with x ranging from 0 to 0.5 were synthesized by solid-state reaction from stoichiometric mixtures of high-purity PbO, SrCO_3 , CaCO_3 , Y_2O_3 , and CuO powders. The powder mixtures were first calcined in air at 800 °C for 30 h and then sintered in argon at 860 °C for 20 h. The crystallinity and phase purity of the samples were checked by x-ray diffraction measurements (XRD; Philips PW 1830; CuK_α radiation). The unit-cell parameters were refined from the XRD data in the $Cmmm$ space group using a Rietveld refinement program FULLPROF. The low level of excess oxygen in the synthesized samples was confirmed by Cu(I)/(II) coulometric titrations.^{20,21} The samples were characterized for superconductivity properties by a superconducting quantum interference device (SQUID) magnetometer (Quantum Design MPMS-5S). The ‘‘effective’’ $T_c^{(e)}$ values were estimated from the χ -versus- T curves, measured in a field-cooling mode under a magnetic field of 10 Oe from room temperature down to 5 K, by extrapolating the diamagnetic portion of the curves to the $\chi = 0$ level.²³ Note that the $T_c^{(e)}$ value is always somewhat lower than the

onset temperature of the Meissner signal, $T_{c,\text{onset}}$, i.e., the temperature that is most typically referred to as T_c .

The x-ray absorption experiments were carried out at the Synchrotron Radiation Research Center (Hsinchu, Taiwan) on the 6-m high-energy spherical grating monochromator beamline. All the measurements were made at room temperature using an ultrahigh vacuum chamber (10^{-9} torr) in order to avoid surface contamination. Furthermore, to minimize the surface contribution, the spectra were recorded by a bulk-sensitive x-ray fluorescence mode with a probing depth of 2000–5000 Å. For the measurement, the sample was finely crushed into powder form and homogeneously spread onto a conducting carbon-based tape. The O K -edge and Cu L_{23} -edge x-ray fluorescence spectra were recorded from the samples using a microchannel plate (MCP) detector system consisting of a dual set of MCP’s with an electrically isolated grid mounted in front of them. The grid was set to a voltage of 100 V, the front of the MCP’s to -2000 V and the rear to -200 V. The grid bias ensured that positive ions did not enter the detector, while the MCP bias ensured that no electrons were detected. The detector was located parallel to the sample surface at a distance of ~ 2 cm. Photons were incident at an angle of 45° with respect to the sample normal. The incident photon flux (I_0) was monitored simultaneously by a Ni mesh located after the exit slit of the monochromator. All the absorption measurements were normalized to I_0 . The photon energies were calibrated with an accuracy of 0.1 eV using the O K -edge absorption peak at 530.1 eV and the Cu L_3 white line at 931.2 eV of CuO reference. The monochromator resolution was set to ~ 0.22 and ~ 0.45 eV at the O $1s$ and Cu $2p$ absorption edges, respectively.

III. RESULTS AND DISCUSSION

The synthesized $(\text{Pb}_{2/3}\text{Cu}_{1/3})_3\text{Sr}_2(\text{Y}_{1-x}\text{Ca}_x)\text{Cu}_2\text{O}_{8+z}$ samples were found to be of the pure $(\text{Pb}_{2/3}\text{Cu}_{1/3})$ -3212 phase within the detection limit of XRD throughout the Ca-substitution range applied, i.e., up to $x = 0.5$. According to the preliminary experiments, the first diffraction peaks that could not be indexed for the $(\text{Pb}_{2/3}\text{Cu}_{1/3})$ -3212 phase appeared at $x \approx 0.6$. Coulometric titrations confirmed that the samples were fully oxygen depleted: within the error limits of the analysis, the amount of excess oxygen z could be considered to be zero for each sample studied. No trend of decreasing oxygen content with increasing the Ca-substitution level was observed. This is in contrast to, e.g., fully oxygenated $\text{Cu}(\text{Ba},\text{Sr})_2(\text{R}_{1-x}\text{Ca}_x)\text{Cu}_2\text{O}_{6+z}$ and $\text{Bi}_2\text{Sr}_2(\text{Y}_{1-x}\text{Ca}_x)\text{Cu}_2\text{O}_{8+\delta}$ systems in which the maximum oxygen content decreases with x .^{20,21,24,25}

The obtained samples possessed an orthorhombic structure within the whole substitution range studied. With an increasing amount of Ca(II) entering the Y(III) site, the lattice parameters a and b were found to decrease, while the c parameter increased (Table I). The expansion of the lattice along the c axis as x increases is related to the fact that the Ca^{2+} ion is larger than the Y^{3+} ion. On the other hand, the concomitant contraction along the a and b axes may be attributed to an increase in the oxidation state of the CuO_2 plane. As x increased in the

TABLE I. The value of $T_c^{(e)}$, the lattice parameters, a , b , and c , and the fitted peak areas of the O K -edge peak at ~ 528.3 eV (I_{528}) and the Cu L_3 -edge peaks at ~ 933.5 eV (I_{933}) [Cu(III)] and ~ 934.5 eV (I_{934}) [Cu(I)] for the $(\text{Pb}_{2/3}\text{Cu}_{1/3})_3\text{Sr}_2(\text{Y}_{1-x}\text{Ca}_x)\text{Cu}_2\text{O}_{8+z}$ ($z \approx 0$) samples.

x	$T_c^{(e)}$ (K)	a (Å)	b (Å)	c (Å)	O K -edge I_{528}	Cu L_3 -edge I_{933}	Cu L_3 -edge I_{934}
0	<5	5.40(1)	5.43(1)	15.74(1)	0.0124	0.0	0.2472
0.1	<5	5.39(1)	5.42(1)	15.73(1)	0.0504	0.0092	0.2744
0.2	19	5.39(1)	5.42(1)	15.75(1)	0.1137	0.0317	0.2939
0.3	16	5.39(1)	5.42(1)	15.76(1)	0.1164	0.0465	0.3054
0.4	60	5.38(1)	5.41(1)	15.76(1)	0.1615	0.0584	0.2537
0.5	60	5.38(1)	5.42(1)	15.77(1)	0.2116	0.0753	0.3018

$(\text{Pb}_{2/3}\text{Cu}_{1/3})_3\text{Sr}_2(\text{Y}_{1-x}\text{Ca}_x)\text{Cu}_2\text{O}_{8+z}$ system bulk superconductivity appeared at $x=0.1\sim 0.2$, and the maximum $T_c^{(e)}$ of about 60 K was obtained at $x=0.4\sim 0.5$ (Table I). Even though the $T_c^{(e)}$ values for the $x=0.4$ and 0.5 samples are the same, judging from the onset temperatures of the Meissner signal the $x=0.5$ sample with $T_{c,\text{onset}}=70$ K is in a slightly overdoped state since for the $x=0.4$ sample, the value of $T_{c,\text{onset}}$ is higher, i.e., 79 K. The somewhat low superconductivity volume fractions and broad superconductivity transition regions, i.e., the difference between the $T_c^{(e)}$ and $T_{c,\text{onset}}$ values, typically observed for the $(\text{Pb}_{2/3}\text{Cu}_{1/3})_3\text{Sr}_2(\text{Y}_{1-x}\text{Ca}_x)\text{Cu}_2\text{O}_{8+z}$ system are attributed to a possibility of some inhomogeneity in the distribution of Ca atoms within the Y sublattice, as first discussed by Marezio.¹⁷

The O K -edge x-ray absorption spectra recorded for the samples in the energy range of 525–555 eV are presented in Fig. 1. For the Ca-free $x=0$ sample the pre-edge area below 532 eV consists of a single peak around 530.4 eV. For the Ca-substituted samples with $0.1 \leq x \leq 0.5$, another pre-edge peak around 528.3 eV develops. The peak at ~ 528.3 eV is assigned to the transition from the O $1s$ state to the O $2p$ hole state in the CuO_2 plane, in line with the interpretations earlier made for the Cu-1212 and Bi-2212 phases.^{2–11} The peak at ~ 530.4 eV might be due to a superposition of O $2p$ hole states in the SrO and PbO-Cu-PbO layers and the upper Hubbard band. The pre-edge peaks were analyzed by fitting with Gaussian functions. Note that, from the spectrum of the $x=0.4$ sample, contribution of two additional small peaks around 535 and 539 eV was subtracted before the fitting. After the subtraction, the shape of $x=0.4$ spectrum was identical with the other spectra. These additional peaks are believed to be due to some impurity from the conducting tape, since the $x=0.4$ sample itself did not differ from the other samples in terms of the phase purity within the detection limits of XRD. The fitting results for the integrated intensity of the pre-edge peak at ~ 528.3 eV, I_{528} , which directly reflects the concentration of holes in the CuO_2 plane, are given in Table I, and also plotted in Fig. 2(a) with increasing Ca content x . The intensity increases continuously within the whole substitution range indicating that the CuO_2 -plane hole concentration also increases continuously as the Ca substitution proceeds. For the exact position of the ~ 528.3 eV pre-edge peak, a weak tendency of decreasing absorption energy

with increasing Ca content is observed, suggesting that the Fermi level shifts to the lower energies with an increasing of the CuO_2 -plane hole concentration. The shift is not, however, as clear as that observed for, e.g., the $\text{Bi}_2\text{Sr}_2(\text{Y}_{1-x}\text{Ca}_x)\text{Cu}_2\text{O}_{8+\delta}$ system with increasing Ca-substitution level.¹¹ Around $x=0.2\sim 0.3$, the I_{528} -versus- x relation shown in Fig. 2(a) exhibits a narrow plateau that might be due to some inhomogeneity in the distribution of Ca at the Y site.¹⁷ Interestingly, this is quite parallel to the trend that applies to the dependence, $T_c^{(e)}$ -versus- x given in Fig. 2(b). Consequently, the $T_c^{(e)}$ -versus- I_{528} relation is rather presented with the bell-shaped line, shown in Fig. 2(c), as typically assumed for the $T_c^{(e)}$ -versus-“ CuO_2 -plane hole concentration” relation of high- T_c superconductors.

The Cu L_{23} -edge spectra in the energy range of 920–960 eV are shown in Fig. 3(a). The spectra were analyzed by fitting the peaks with Gaussian functions, as demonstrated

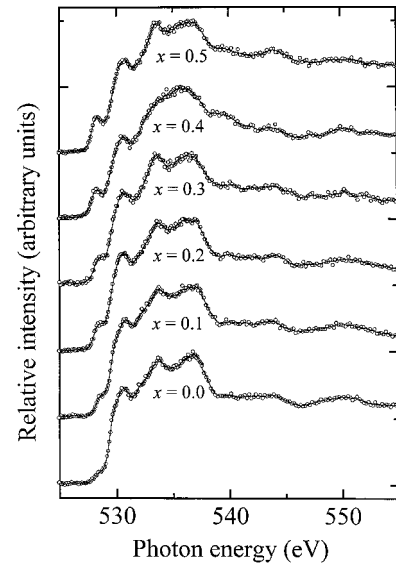


FIG. 1. The O K -edge XANES spectra for the $(\text{Pb}_{2/3}\text{Cu}_{1/3})_3\text{Sr}_2(\text{Y}_{1-x}\text{Ca}_x)\text{Cu}_2\text{O}_{8+z}$ samples with $x=0-0.5$ in the energy range of 525–555 eV. Note that, the slightly different shape of the $x=0.4$ spectrum is due to some small impurity from the conducting tape used as a sample holder. These impurity peaks centered at around 535 eV and 539 eV were subtracted from the spectrum before the fitting.

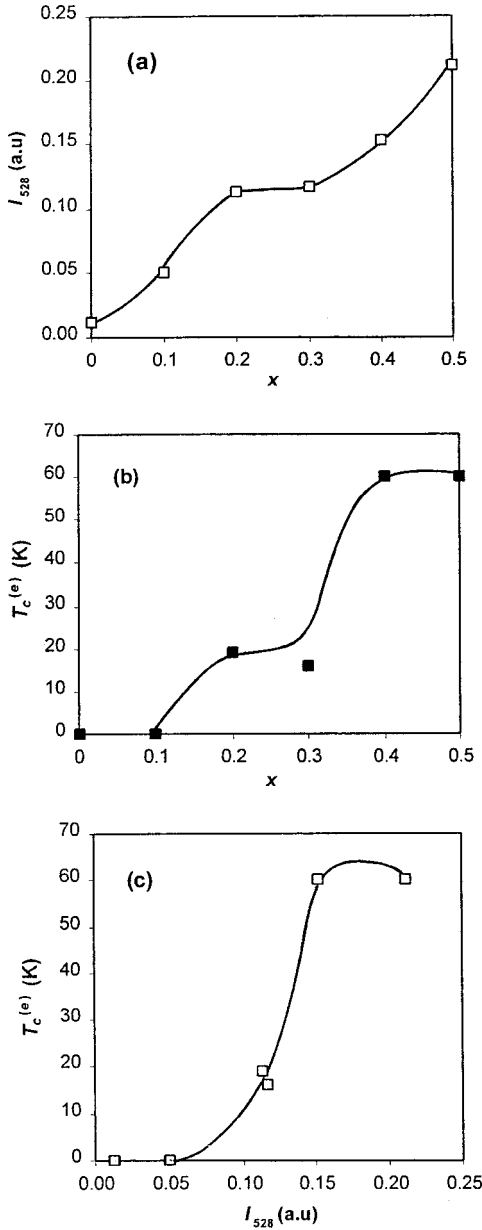


FIG. 2. Various correlations between the Ca-substitution level, x , the integrated intensity of the O K -edge XANES pre-edge peak at ~ 528.3 eV, I_{528} , and the value of $T_c^{(e)}$ for the $(\text{Pb}_{2/3}\text{Cu}_{1/3})_3\text{Sr}_2(\text{Y}_{1-x}\text{Ca}_x)\text{Cu}_2\text{O}_{8+z}$ samples: (a) I_{528} -versus- x , (b) $T_c^{(e)}$ -versus- x , and (c) $T_c^{(e)}$ -versus- I_{528} . Note that, the value of I_{528} is in arbitrary units.

for the spectra of the $x=0$ and 0.5 samples in Fig. 3(b). The results are given in Table I. Two narrow peaks centered at ~ 932.0 and ~ 952.0 eV dominate the spectra of all the six samples. These peaks are due to formally divalent copper states, i.e., transitions from the Cu $(2p_{3/2})3d^9$ ground states into the Cu $(2p_{3/2})3d^{10}$ excited states, where $(2p_{3/2})$ denotes a $2p_{3/2}$ or $2p_{1/2}$ hole. With an increasing degree of Ca substitution, a feature due to the formally trivalent copper in the CuO_2 plane appears on the high-energy side of the 932.0 eV peak. This high-energy shoulder at ~ 933 eV, reported for the first time for the $\text{CuBa}_2\text{YCu}_2\text{O}_{6+z}$

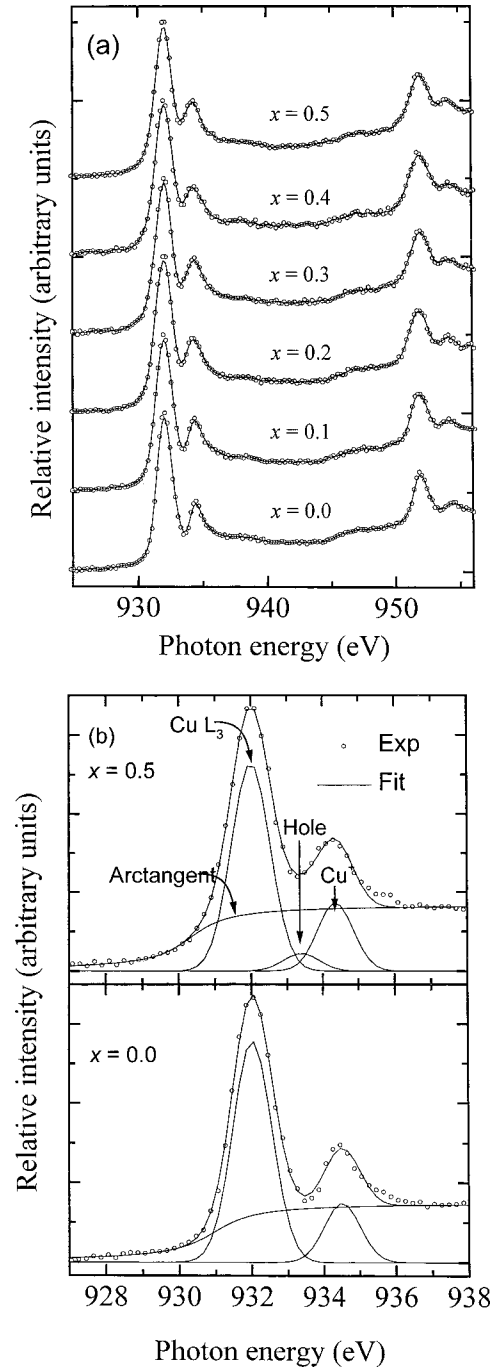


FIG. 3. (a) The Cu L_{23} -edge XANES spectra for the $(\text{Pb}_{2/3}\text{Cu}_{1/3})_3\text{Sr}_2(\text{Y}_{1-x}\text{Ca}_x)\text{Cu}_2\text{O}_{8+z}$ samples with $x=0-0.5$ in the energy range 920–960 eV, and (b) the fitting of the spectra of the $x=0$ and 0.5 samples with Gaussian components.

phase as a consequence of oxygen doping,²⁷ has been interpreted as transitions from the Cu $(2p_{3/2})3d^9L$ ground states into the Cu $(2p_{3/2})3d^{10}L$ excited states, where L denotes a ligand hole in the O $2p$ orbital. With an increasing Ca-substitution level, the 932.0 eV peak becomes increasingly asymmetric, indicating that the amount of formally trivalent copper continuously increases (Table I). However, as compared to the fully-oxygenated $\text{CuBa}_2\text{YCu}_2\text{O}_{6+z}$ ($z \approx 1$) phase, the shoulder is less prominent even in the spectrum of the

most heavily substituted sample ($x=0.5$). This is due to the fact that in $(\text{Pb}_{2/3}\text{Cu}_{1/3})_3\text{Sr}_2(\text{Y}_{1-x}\text{Ca}_x)\text{Cu}_2\text{O}_{8+z}$ with $z \approx 0$, only the CuO_2 -plane copper is in an oxidation state higher than +II, while in $\text{CuBa}_2\text{YCu}_2\text{O}_{6+z}$ with $z \approx 1$, not only the CuO_2 plane but also the CuO_z chain contains formally trivalent copper atoms.

In the Cu L₂₃-edge spectra, an additional peak around 934.5 eV, characteristically observed in monovalent copper compounds,²⁶ is seen for all the samples studied. This peak arises from the Cu $3d_{z^2-2p_z}$ hybrids between the charge-reservoir copper atom and the PbO-layer oxygen atom. The intensity of the 934.5 eV peak remains essentially unchanged upon increasing the Ca-substitution level (Table I), revealing that the holes generated through the Ca(II)-for-Y(III) substitution are not transferred to the charge-reservoir copper atom, but remain solely in the CuO_2 plane.

The present XANES results clearly established that in Ca-substituted oxygen-depleted $(\text{Pb}_{2/3}\text{Cu}_{1/3})$ -3212, copper atoms with oxidation states below and above +II coexist in the same structure: the CuO_2 -plane Cu is in the mixed +II/+III state while the charge-reservoir Cu possesses a twofold linear coordination to the nearest PbO-layer oxygen atoms and is monovalent (cf. charge-reservoir Cu in $\text{CuBa}_2\text{RCu}_2\text{O}_6$). This conclusion is consistent with charge-balance considerations and the results of BVS calculations^{15,17,19} and chemical analyses.^{20,21} Note that, the Pb atom with five nearest-neighbor oxygen atoms is believed to be divalent.^{20,21} That the CuO_2 plane can keep the holes created through Ca substitution violates against the redox-potential scheme: based on the redox potentials of the Pb(II)/(IV), Cu(I)/(II) and Cu(II)/(III) couples, Pb(II) and Cu(I) should be oxidized more easily than Cu(II). In a solid matrix, however, the redox-potential scheme applies only when the number of nearest-neighbor counter ions allows the predicted changes in the oxidation state. The fact that in the oxygen-depleted $(\text{Pb}_{2/3}\text{Cu}_{1/3})$ -3212 phase, the coordination numbers of the charge-reservoir Cu and Pb atoms are low, i.e., 2 and 5, respectively, is thus crucially important in terms of facilitating the hole doping of the CuO_2 plane. At the twofold/fivefold coordination Cu/Pb cannot be oxidized beyond the oxidation state +I/+II. On the other hand, the incorporation of oxygen in the Ca-substituted $(\text{Pb}_{2/3}\text{Cu}_{1/3})$ -3212 phase would kill the superconductivity by increasing the coordination numbers of the charge-reservoir Cu and Pb atoms and thereby enabling the CuO_2 -plane holes to move to the PbO-CuO₂-PbO charge-reservoir block.^{17,20,21}

Finally, it is interesting to compare the effectiveness of Ca substitution in oxygen-depleted $(\text{Pb}_{2/3}\text{Cu}_{1/3})$ -3212 in terms of increasing the CuO_2 -plane hole concentration and thereby the value of T_c^e to data previously obtained for other M - $m2(n-1)n$ phases with a two- CuO_2 -plane structure, i.e., $n=2$. In Fig. 4, the value of T_c^e is plotted against the Ca-substitution level x for the present $(\text{Pb}_{2/3}\text{Cu}_{1/3})_3\text{Sr}_2(\text{Y}_{1-x}\text{Ca}_x)\text{Cu}_2\text{O}_{8+z}$ ($z \approx 0$) system together with the systems, $\text{Cu}(\text{Ba}_{0.8}\text{Sr}_{0.2})_2(\text{Yb}_{1-x}\text{Ca}_x)\text{Cu}_2\text{O}_{6+z}$ (Cu-1212; $z \approx 0$),^{10,24,28} and $\text{Bi}_2\text{Sr}_2(\text{Y}_{1-x}\text{Ca}_x)\text{Cu}_2\text{O}_{8+\delta}$ (Bi-2212; δ decreases from 0.52 to 0.26 with an increase of x from 0 to 1).^{20,25} In the

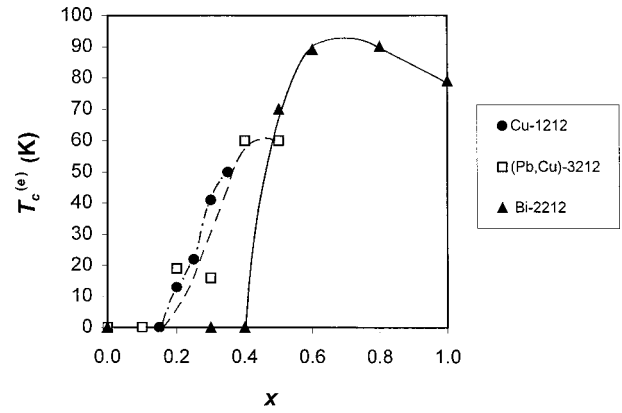


FIG. 4. The T_c^e -versus- x relation for the systems, $(\text{Pb}_{2/3}\text{Cu}_{1/3})_3\text{Sr}_2(\text{Y}_{1-x}\text{Ca}_x)\text{Cu}_2\text{O}_{8+z}$ with $z \approx 0$ (□), $\text{Cu}(\text{Ba}_{0.8}\text{Sr}_{0.2})_2(\text{Yb}_{1-x}\text{Ca}_x)\text{Cu}_2\text{O}_{6+z}$ with $z \approx 0$ (●), and $\text{Bi}_2\text{Sr}_2(\text{Y}_{1-x}\text{Ca}_x)\text{Cu}_2\text{O}_{8+\delta}$ with δ decreasing from 0.52 to 0.26 with x increasing from 0 to 1 (▲).

case of the Bi-2212 system with a strongly oxygenated $\text{BiO}_{1+\delta'}$ - $\text{BiO}_{1+\delta'}$ charge reservoir, quite a high Ca substitution level is required for the appearance of superconductivity, i.e., $x \approx 0.5$ (Fig. 4). This is due to two different factors: by means of redox-chemical analyses it has been shown that with increasing x (i) the oxygen content decreases, and (ii) the valence of Bi increases.^{1,20,21,25} In other words, each Ca atom entering the structure produces on average less than one electron hole since the concomitant decrease in the oxygen content partially counteracts the effects of the divalent-for-trivalent substitution. Furthermore, the produced holes are not quantitatively directed into the CuO_2 plane but are partly accommodated in the $\text{BiO}_{1+\delta'}$ - $\text{BiO}_{1+\delta'}$ charge reservoir. On the other hand, in the $(\text{Pb}_{2/3}\text{Cu}_{1/3})$ -3212 and Cu-1212 systems with the oxygen-depleted charge reservoirs, PbO-Cu-PbO and Cu, respectively, the holes produced by means of Ca substitution are directed efficiently into the CuO_2 plane. Consequently, superconductivity appears, as seen in Fig. 4, at a much lower Ca content of $x \approx 0.2$ than in the case of the Bi-2212 phase.

IV. CONCLUSION

By means of O K-edge and Cu L₂₃-edge XANES measurements it has been directly established that the holes generated through the Ca(II)-for-Y(III) substitution in the oxygen-depleted $(\text{Pb}_{2/3}\text{Cu}_{1/3})_3\text{Sr}_2(\text{Y}_{1-x}\text{Ca}_x)\text{Cu}_2\text{O}_{8+z}$ phase are solely transferred into the CuO_2 plane. As a manifestation for the increase in the CuO_2 -plane hole concentration, two indicative features appeared in the measured O K-edge and Cu L₂₃-edge absorption spectra, i.e., the pre-edge peak at ~ 528.3 eV in the former and the high-energy shoulder of the 932.0 eV main peak in the latter spectra. On the other hand, the fact that the intensity of the 934.5 eV peak in the Cu L₂₃-edge spectra remained unchanged confirmed that the charge-reservoir Cu atom is not oxidized upon the Ca substitution. The present XANES results are in good agreement with the charge-distribution scheme proposed for the $(\text{Pb}_{2/3}\text{Cu}_{1/3})_3\text{Sr}_2(\text{Y}_{1-x}\text{Ca}_x)\text{Cu}_2\text{O}_{8+z}$ system in previous

works based on structural considerations and wet-chemical analysis.

ACKNOWLEDGMENTS

T. Nakane is thanked for his help in the SQUID measurements. The present paper has been supported by a Grant-in-

Aid for Scientific Research (Contract No. 1305002) from the Ministry of Education, Science, and Culture of Japan, by an International Collaborative Research Project Grant-2000 of Materials and Structures Laboratory, Tokyo Institute of Technology, and by the Academy of Finland (Decision No. 46039).

*Present address: Materials and Structures Laboratory, Tokyo Institute of Technology, Yokohama 226-8503, Japan.

- ¹M. Karppinen and H. Yamauchi, *Mater. Sci. Eng., R.* **26**, 51 (1999).
- ²N. Nücker, E. Pellegrin, P. Schweiss, J. Fink, S. L. Molodtsov, C. T. Simmons, G. Kaindl, W. Frentrup, A. Erb, and G. Müller-Vogt, *Phys. Rev. B* **51**, 8529 (1995).
- ³M. Merz, N. Nücker, E. Pellegrin, P. Schweiss, S. Schuppler, M. Kielwein, M. Knupfer, M. S. Golden, J. Fink, C. T. Chen, V. Chakarian, Y. U. Idzerda, and A. Erb, *Phys. Rev. B* **55**, 9160 (1997).
- ⁴M. Merz, N. Nücker, P. Schweiss, S. Schuppler, C. T. Chen, V. Chakarian, J. Freeland, Y. U. Idzerda, M. Kläser, G. Müller-Vogt, and Th. Wolf, *Phys. Rev. Lett.* **80**, 5192 (1998).
- ⁵J. M. Chen, R. G. Liu, S. C. Chung, R. S. Liu, M. J. Kramer, K. W. Dennis, and R. W. McCallum, *Phys. Rev. B* **55**, 3186 (1997).
- ⁶J. M. Chen, R. S. Liu, J. G. Lin, C. Y. Huang, and J. C. Ho, *Phys. Rev. B* **55**, 14 586 (1997).
- ⁷R. S. Liu, C. Y. Chang, and J. M. Chen, *Inorg. Chem.* **37**, 5527 (1998).
- ⁸R. S. Liu, C. Y. Chang, J. M. Chen, and R. G. Liu, *Supercond. Rev.* **11**, 563 (1998).
- ⁹J. M. Chen, R. S. Liu, P. Nachimuthu, M. J. Kramer, K. W. Dennis, and R. W. McCallum, *Phys. Rev. B* **59**, 3855 (1999).
- ¹⁰M. Karppinen, H. Yamauchi, T. Nakane, K. Fujinami, K. Lehmus, P. Nachimuthu, R. S. Liu, and J. M. Chen (unpublished).
- ¹¹I. J. Hsu, R. S. Liu, J. M. Chen, R. G. Liu, L. Y. Jang, J. F. Lee, and K. D. M. Harris, *Chem. Mater.* **12**, 1115 (2000).
- ¹²R. J. Cava, B. Batlogg, J. J. Krajewski, L. W. Rupp, L. F. Schneemeyer, T. Siegrist, R. B. van Dover, P. Marsh, W. F. Peck, Jr., P. K. Gallagher, S. H. Glarum, J. H. Marshall, R. C. Farrow, J. V. Waszczak, R. Hull, and P. Trevor, *Nature (London)* **336**, 211 (1988).
- ¹³M. A. Subramanian, J. Gopalakrishnan, C. C. Torardi, P. L. Gai, E. D. Boyes, T. R. Askew, R. B. Flippen, W. E. Farneth, and A. W. Sleight, *Physica C* **157**, 124 (1989).
- ¹⁴M. Marezio, P. Bordet, J. J. Capponi, R. J. Cava, C. Chaillout, J. Chevanas, A. W. Hewat, J. L. Hodeau, and P. Strobel, *Physica C* **162-164**, 281 (1989).
- ¹⁵M. Marezio, A. Santoro, J. J. Capponi, E. A. Hewat, R. J. Cava, and F. Beech, *Physica C* **169**, 401 (1990).
- ¹⁶P. Bordet, J. J. Capponi, J. L. Hodeau, M. Marezio, R. J. Cava, A. W. Hewat, E. A. Hewat, and A. Santoro, *Eur. J. Solid State Inorg. Chem.* **27**, 57 (1990).
- ¹⁷M. Marezio, *Acta Crystallogr., Sect. A: Found. Crystallogr.* **47**, 640 (1991).
- ¹⁸T. Karlemo, M. Karppinen, L. Niinistö, J. Lindén, and M. Lippmaa, *Physica C* **292**, 225 (1997).
- ¹⁹M. Karppinen and H. Yamauchi, *Philos. Mag. B* **79**, 343 (1999).
- ²⁰M. Karppinen, A. Fukuoka, J. Wang, S. Takano, M. Wakata, T. Ikemachi, and H. Yamauchi, *Physica C* **208**, 130 (1993).
- ²¹M. Karppinen, A. Fukuoka, L. Niinistö, and H. Yamauchi, *Supercond. Sci. Technol.* **9**, 121 (1996).
- ²²R. J. Cava, M. Marezio, J. J. Krajewski, W. F. Peck, Jr., A. Santoro, and F. Beech, *Physica C* **157**, 272 (1989).
- ²³T. Matsushita, A. Matsuda, and K. Yanagi, *Physica C* **213**, 477 (1993).
- ²⁴K. Fujinami, M. Karppinen, and H. Yamauchi, *Physica C* **300**, 17 (1998).
- ²⁵M. Kotiranta, T. Nakane, M. Karppinen, H. Yamauchi, and L. Niinistö, *J. Low Temp. Phys.* **117**, 839 (1999).
- ²⁶M. Grioni, J. B. Goedkoop, R. Schoorl, F. M. F. de Groot, J. C. Fuggle, F. Schäfers, E. E. Koch, G. Rossi, J.-M. Esteve, and R. C. Karnatak, *Phys. Rev. B* **39**, 1541 (1989).
- ²⁷A. Bianconi, M. DeSantis, A. Di Ciccio, A. M. Flank, A. Fronk, A. Fontaine, P. Legarde, H. K. Yoshida, A. Kotani, and A. Marcelli, *Phys. Rev. B* **38**, 7196 (1988).
- ²⁸M. Karppinen, H. Yamauchi, K. Fujinami, T. Nakane, K. Peitola, H. Rundlöf, and R. Tellgren, *Phys. Rev. B* **60**, 4378 (1999).